HHS Public Access

Author manuscript

Nat Chem Biol. Author manuscript; available in PMC 2018 March 11.

Published in final edited form as:

Nat Chem Biol. 2017 November ; 13(11): 1155–1157. doi:10.1038/nchembio.2471.

Oxidative cyclization of prodigiosin by an alkylglycerol monooxygenase-like enzyme

Tristan de Rond[1], **Parker Stow**[1], **Ian Eigl**[2], **Rebecca E Johnson**[1], **Leanne Jade G Chan**[3], **Garima Goyal**[3], **Edward EK Baidoo**[3], **Nathan J Hillson**[3,4], **Christopher J Petzold**[3], **Richmond Sarpong**[1], and **Jay D Keasling**[2,3,5,6]

[1]Department of Chemistry, University of California, Berkeley, California 94720, United States

[2]Department of Chemical and Biomolecular Engineering, University of California, Berkeley, California 94720, United States

[3]DOE Joint BioEnergy Institute, Emeryville, California 94608, United States, and Biological Systems and Engineering Division, Lawrence Berkeley National Lab, Berkeley, California 94720, United States

[4]DOE Joint Genome Institute, Walnut Creek, California 94598, United States

[5]Department of Bioengineering and California Institute for Quantitative Biosciences, University of California, Berkeley, California 94720, United States

[6]Novo Nordisk Foundation Center for Biosustainability, Technical University of Denmark, Hørsholm, Denmark

Abstract

Prodiginines, tripyrrole alkaloids displaying a wide array of bioactivities, occur as linear and cyclic congeners. Identification of an unclustered biosynthetic gene led to the discovery of the enzyme responsible for catalyzing the regiospecific C–H activation and cyclization of prodigiosin to form cycloprodigiosin in *Pseudoalteromonas rubra*. This enzyme is closely related to alkylglycerol monooxygenase, and unrelated to RedG, the Rieske oxygenase that produces cyclized prodiginines in *Streptomyces*, implying convergent evolution.

The prodiginines are a family of red tripyrrole natural products that display a broad range of promising medicinal properties including antimalarial, anticancer, and immunosuppressive activities[1–3]. Notably, they have been shown to induce apoptosis in cancer cells while leaving nonmalignant cells unaffected[3–5]. Most prodiginines occur in linear and cyclic forms

Author contributions

T.dR., R.E.J., R.S., and J.D.K. conceived of the study. T.dR., P.S. and I.E. constructed plasmids and performed microbiological manipulations and extractions, R.E.J. performed synthetic organic chemistry. T.dR., E.E.K.B., and C.J.P. performed analytical chemistry, L.J.G.C. and C.J.P. performed proteomic analysis, and G.G. and N.J.H. PCR amplified and purified DNA fragments. T.dR. performed bioinformatic analysis. All authors contributed to the manuscript.

Competing financial interests

The authors declare no competing financial interests.

with respect to their aliphatic tails, which is apparent in prodigiosin (**1**) versus cycloprodigiosin (**2**), and undecylprodigiosin versus streptorubin B (Fig. 1). It has been proposed that these carbocycles bias the molecules towards their biologically active conformations[6]. For instance, when tested for antimicrobial activity, the cyclic prodiginine **2** was found to be more active against a variety of bacteria than its straight-chain congener **1**[7].

The biosynthesis of cyclic prodiginines proceeds by oxidative cyclization of their respective linear congeners (Fig. 1a). The enzymes catalyzing the cyclization reactions to produce streptorubin B, metacycloprodigiosin, marineosin and roseophilin in various *Streptomyces spp.* all belong to a family of Rieske oxygenases represented by *Streptomyces coelicolor* RedG (Fig. 1c)[8–11]. The remarkable catalytic capacities of these enzymes have been employed to synthesize natural and unnatural cyclic prodiginines[10–12]. However, to date, no enzyme catalyzing the cyclization of **1** into **2** has been identified. Given the difficulty of realizing regiospecific C–H activation using traditional synthetic methods, additional enzymes catalyzing such oxidative cyclizations would be a welcome expansion of the biocatalytic toolbox. Here, we identify the enzyme responsible for the regiospecific C–H activation and cyclization of **1** in the marine bacterium *Pseudoalteromonas rubra*, which is known to produce both **1** and **2**. The enzyme is unrelated to RedG, but is rather a member of the FA_hydroxylase integral membrane di-iron oxygenase family, and is closely related to metazoan alkylglycerol monooxygenase.

The biosynthesis of **1** has been thoroughly studied in *Serratia spp.*, where the *pig* (for “pigment”) gene cluster encodes the enzymes responsible for biosynthesis of **1**[13,14]. Apart from *pigK* and *pigN*, whose precise roles remain uncharacterized, the function of each *pig* gene has been elucidated. The biosynthesis of **1** has been shown to proceed through a bifurcated pathway (Fig. 1a). PigBDE biosynthesize 2-methyl-3-amylpyrrole (MAP, **3**), while PigA and PigF–N form 4-methoxy-2,2′-bipyrrole-5-carboxaldehyde (MBC, **4**). These two intermediates are condensed by PigC to yield **1**. We expected the biosynthesis of **1** to proceed similarly in *P. rubra*, given that its genome[15] harbors a biosynthetic cluster showing high sequence identity with the *Serratia* ATCC39006 *pig* cluster (Fig. 1b and Supplementary Results, Supplementary Table 1).

We first set out to ensure that cyclization is the final step in cyclic prodiginine biosynthesis in *P. rubra*, as is the case in *S. coelicolor*[8] (Fig. 1c). To this end, we constructed an in-frame Δ*pigE* mutant of *P. rubra* which, as expected, produced neither **1** nor **2**. Upon feeding it **1**, we were able to detect **2** using LC-MS (Supplementary Fig. 1). These results confirmed that, like in *S. coelicolor*, the cyclization of **1** in *P. rubra* can occur as the final step in **2** biosynthesis. Further support for this model is the observation that recombinant *E. coli* expressing *P. rubra pigBCDE* produces **1** but not **2** upon feeding with synthetic **4** (Fig. 2a and Supplementary Fig. 2).

Bioinformatic analysis of the *P. rubra* genome[15] revealed no *redG* homologs, and the only genes encoding enzymes homologous to oxidases found in the *pig* cluster were those already ascribed to steps in the **1** biosynthesis pathway. Upon examining the *P. rubra pig* cluster for genes not present in *Serratia* (which does not produce **2**), we noticed that while the two clusters show near-perfectly conserved synteny, the *P. rubra* cluster actually lacks a *pigN*

gene (Fig. 1b). We thus searched the *P. rubra* genome for *pigN* homologs. While no close *pigN* homologs could be found, we did detect a homolog of *S. coelicolor redF*—which is thought to fulfill the role of *pigN* in *S. coelicolor*[13,14]—in the *PRUB675* locus. (For a more in-depth analysis of the relationship between these proteins, which are all in the DUF_1295 protein family, see Supplementary Fig. 3). In *Serratia*, disruption of *pigN* impedes but does not abolish conversion of 4-hydroxy-2,2′-bipyrrole-5-carboxaldehyde (HBC, **5**) into **4**. Accumulation of **5** results in diminished production of **1** and increased production of norprodigiosin (**6**), which is formed by the PigC-catalyzed condensation of **5** with **3**[16]. The same phenotype was observed for *P. rubra ΔPRUB675*, suggesting that *PRUB675* fulfills the function of *pigN* in *P. rubra* (Supplementary Fig. 4).

Analysis of the gene neighborhood of *PRUB675* revealed that the gene appears to be part of a transcriptional unit with *PRUB680*, which bears homology to di-iron oxygenases. Deleting *PRUB680* in *P. rubra* abolished production of **2**, while **1** was left unaffected (Fig. 2a). Furthermore, heterologous expression of *PRUB680* alongside *pigBCDE* in *E. coli* fed 4 led to the formation of **2**. Direct bioconversion of **1** to **2** by recombinant *E. coli* could only barely be observed, which has also been found to be the case for the bioconversion of undecylprodigiosin to streptorubin B by *Streptomyces* expressing *redG*[8]. We suspect that **1** is unable to cross the *E. coli* cell wall effectively, while **4** can.

Bioinformatic analysis showed that PRUB680 shares no significant sequence similarity with RedG, and is instead a member of the FA_hydroxylase family of integral membrane di-iron oxygenases. PRUB680 displays the characteristic eight-histidine motif that is essential for iron binding and catalysis in this enzyme family (Supplementary Fig. 5)[17,18]. Di-iron oxygenases are known to carry out a wide variety of C–H activation chemistries (Supplementary Figs. 6 and 7, and Supplementary Table 2)[17], but so far none have been reported to catalyze oxidative cyclization or C–C bond formation[19].

The closest characterized homolog of PRUB680 is alkylglycerol monooxygenase (AGMO), which is present only in metazoans and some protists, and forms an isolated eukaryotic branch of the FA_hydroxylase family. AGMO plays a central role in lipid homeostasis by catalyzing the breakdown of ether lipids, a deficit of which leads to the development of cataracts and disrupts spermatogenesis in mice[20]. AGMO is distinct among di-iron oxygenases—most of which obtain their reducing equivalents from nicotinamide cofactors—in that it utilizes pterin cofactors, which are thought to bind in a pocket on the cytosolic side of this transmembrane protein[21]. To ensure that a possible analogous pocket in PRUB680 would be accessible to exogenously added reducing cofactors, we pursued the *in vitro* characterization of PRUB680 in inverted membrane vesicles, generated via sonication of *E. coli* spheroplasts[22]. Under these conditions, we were able to observe PRUB680-catalyzed conversion of **1** to **2**. Like AGMO, PRUB680 appeared to require pterin cofactors to supply its reducing equivalents, accepting various pterins equally well (Fig. 2b). Nicotinamide and flavin cofactors were not accepted.

PRUB680 was inhibited by EDTA, but activity could be recovered by iron supplementation (Fig. 2b), suggesting that, like all other characterized members of the FA_hydroxylase family, PRUB680 utilizes iron to achieve catalysis. Copper and vanadium—other metals

known to facilitate enzymatic C–H activation[19]—could not recover activity. On the basis of the mechanistic analysis of other di-iron enzymes[17,18], we propose that the cyclization of **1** proceeds by abstraction of an aliphatic hydrogen followed by addition of the radical into the tripyrrole π system (Supplementary Fig. 8).

Besides the functional similarity between PRUB680 and AGMO, these enzymes' catalytic domains share 43% sequence identity (Supplementary Fig. 9), and are predicted to have the same nine-transmembrane topology (Supplementary Fig. 5)[21]. Since thus far all efforts to express AGMO in microbial hosts have been unsuccessful[20,23], PRUB680 may serve as a convenient model system for the biochemical characterization of this enzyme.

PRUB680 resides in a predominantly prokaryotic clade of the FA_hydroxylase protein family (Fig. 6) which, considering the remarkable catalytic diversity displayed by the few members characterized so far, may contain many enzymes catalyzing novel C–H activation reactivity. Moreover, some of these unexplored enzymes may be involved in C–H activating steps in the biosynthesis of novel natural products. None of PRUB680's closest homologs are found in organisms known to produce prodiginines (Supplementary Fig. 7), suggesting that PRUB680 is a functional outlier among enzymes that carry out other oxidative chemistry. The genomic context of these homologs of gives no clear indication regarding their functions (Supplementary Table 3).

Most characterized bacterial biosynthetic pathways are encoded by genes physically clustered on the genome. However, in *P. rubra*, the genes encoding prodiginine biosynthesis are split across two loci, a situation we were alerted to by the absence of the strictly conserved gene *pigN*. An analogous strategy may help to identify biosynthetic enzymes in other organisms that are not clustered with their respective pathways.

The exact role of PigN in prodiginine biosynthesis is still unknown. Given that PigB—which catalyzes the final step of **3** biosynthesis—is predicted to have two transmembrane helices (Supplementary Fig. 10), and the condensing enzyme PigC has been found to localize to the membrane when expressed heterologously[24], we suspect that the concluding steps of **1** biosynthesis occur at the membrane. PigN has five predicted transmembrane helices (Supplementary Fig. 11) and might act to recruit PigF to the membrane. The presence of *pigN* (or *redF*) is strictly conserved among prodiginine-producing organisms, despite the weak phenotype of Δ*pigN* merely changing the ratio of **1** to **6**. *P. rubra* may have acquired *pigA–M* in one horizontal gene transfer event, while acquiring *PRUB675–680* independently, perhaps due to strong selective pressure for a gene fulfilling the role of *pigN*.

In summary, we have shown that PRUB680, a membrane di-iron oxygenase-like enzyme, produces **2** by cyclization of **1**, analogous to the cyclization of undecylprodigiosin to form streptorubin B catalyzed by RedG, a Rieske oxygenase-like enzyme. Despite sharing no sequence similarity, both enzymes are predicted to employ histidine-ligated non-heme iron centers[18,25] to catalyze the oxidative cyclization of prodiginines. PRUB680 bears strong homology to AGMO and has similar cofactor requirements, and hence may serve as a prokaryotic model for the latter. Furthermore, the large supply of uncharacterized bacterial enzymes related to PRUB680 may provide a valuable source of novel C–H activation

reactivity. PRUB680 itself may also prove useful as a biocatalyst to produce novel prodiginines, as RedG has. The fact that cyclic prodiginine biosynthesis evolved independently at least twice suggests that there exists a strong selective pressure to produce cyclic prodiginines. However, thus far the ecological role of the prodiginines—and hence the adaptive advantage conferred by cyclic prodiginines—remains an enigma.

Online methods

Synthetic chemistry

Cycloprodigiosin (**2**)[26] and MBC (**4**)[27] were synthesized as described previously.

Bacterial cultivation

E. coli was propagated at 37 °C on LB agar or in LB broth. For the cultivation of *P. rubra* (at 30 °C), these media were supplemented with 10% v/v 180 g/L Instant Ocean Sea Salt (IO) (Spectrum Brands, Blacksburg, VA), autoclaved separately. Descriptions of bacterial strains employed in this study are provided in Supplementary Table 4.

Plasmid construction

DNA assembly protocols were designed using j5 and DeviceEditor software[28]. Descriptions of plasmids employed in this study are provided in Supplementary Table 5. Assembly of DNA fragments (Supplementary Table 6) was performed using NEBuilder HiFi DNA Assembly Master Mix or NEB Golden Gate Assembly Mix (NEB) per manufacturer's directions. The 11 kb *pigBCDE* fragment was cloned behind a T7 promoter using the Zero Blunt TOPO PCR Cloning Kit (ThermoFisher).

Targeted gene disruptions in *P. rubra*

We employed conjugative transfer of a suicide plasmid following literature precedent[29], however, counterselection with SacB was not effective in our hands. This held true even with *sacB* under the control of promoters expressed highly in *P. rubra*, as determined by shotgun proteomics (Supplementary Table 7). Instead, we replaced *sacB* with *lacZ* and identified double crossovers by blue-white screening (Supplementary Fig. 12). *E. coli* WM3064 was transformed with suicide vectors conferring both erythromycin and chloramphenicol resistance markers under the control of the *P. rubra* elongation factor G (*PRUB9669* on contig 67) promoter, the *P. rubra* 30S ribosomal protein S13 promoter (*PRUB13406* on contig 115, this is actually a polycistronic locus with a number of ribosomal proteins and an RNA polymerase subunit) driving *lacZ*, and ~1 kb regions homologous to those upstream and downstream of the target. After overnight growth on LB agar with 25 μg/mL chloramphenicol, 100 μM X-gal, and 300 μM diaminopimelic acid (DAP), a colony was patched directly on LB agar with 4% v/v 180 g/L IO and 300 μM DAP, with a wild-type *P. rubra* colony patched on top. After conjugating at 30 °C overnight, the patch was struck out for single colonies on LB agar with 10% v/v 180 g/L IO, 25 μg/mL erythromycin, and 500 μM X-gal. Blue colonies (single-crossovers) were passaged until homogeneous. These were then sub-cultured on the same growth media without erythromycin, and white colonies were isolated and confirmed to be sensitive to erythromycin. To distinguish double-crossovers from revertants, colony PCR was performed by picking colonies into neat DMSO, diluting

1:10 with water and using that as template (1% v/v) with 5Prime HotMasterMix polymerase and primers as specified in Supplementary Table 6.

Prodiginine production in *P. rubra*

P. rubra was grown in 50 mL 20% v/v LB, 10% v/v 180 g/L Instant Ocean, 70% de-ionized water, in a 250 mL baffled shake flask. After 12 hours of growth at 30 °C, 2 mL of the culture was extracted with 3 mL 1:1 chloroform:methanol. The organic layer was evaporated to dryness, dissolved in ethanol, diluted 1:1 in de-ionized water, and analyzed by LC-MRM-MS and LC-TOF-MS.

Heterologous prodiginine production in *E. coli*

E. coli BLR (DE3) was transformed with plasmids containing *pigBCDE* and either *PRUB680* or RFP. Overnight cultures were diluted 1:10 into LB supplemented with 50 μg/mL kanamycin and 25 μg/mL chloramphenicol and grown at 37 °C to an OD_{600} of 0.6, upon which they were induced with 100 μM IPTG at 30 °C for 16 h. 10 mL of cells were harvested by centrifugation (8,000 g, 5 min), resuspended in 300 μL of LB medium, and spread onto agar plates with 0.1 mM IPTG and antibiotics as before. 10 μL of 1 mM MBC in 1:3 DMSO:water was spotted onto the plates, which were left to grow overnight at 30 °C. The pink halo (as can be seen in Supplementary Fig. 2) was scraped off and resuspended in 1 mL de-ionized water with 2% TFA by vigorous vortexing. The cell suspension was extracted with 2 mL of 1:1 v/v chloroform:methanol. The organic layer was evaporated to dryness dissolved in ethanol, diluted 1:1 in de-ionized water, and analyzed by LC-MRM-MS.

In vitro analysis of PRUB680 in inverted *E. coli* membrane vesicles

An overnight culture of *E. coli* BLR (DE3) containing pET28-PRUB680 was diluted 1:10 into 3 × 500 mL LB supplemented with 50 μg/mL kanamycin in 2 L baffled flasks and grown at 37 °C. When the cells reached an OD_{600} of 0.6, the flasks were cooled to 18 °C and induced with 100 mM IPTG for 3 h. The cells were harvested by centrifugation (5,000 g, 10 min), washed with 30 mL spheroplasting buffer (30% sucrose, 200 mM Tris·HCl pH 8.0, 2mM EDTA) and incubated rocking for 30 min at room temperature in 30mL spheroplasting buffer + 3 mg lysozyme. Spheroplasts were harvested by centrifugation (5,000 g, 10 min), resuspended in 30 mL assay buffer (100 mM HEPES·KOH pH 7.8, 50 mM K_2SO_4, 1% v/v Sigma Protease Inhibitor Cocktail P8849), divided into 20 × 1.5 mL in 2 mL centrifuge tubes, and sonicated in a cup-horn sonicator (Qsonica Q700 with 431MPX horn, Amplitude: 75%, 1 min on, 1 min off) for 45 min. of total “on” time. The water bath temperature was maintained between 3 and 10 °C. The tubes were centrifuged at 12,000 g for 10 min at 4 °C, the supernatants combined and again centrifuged at 12,000 g for 10 min at 4 °C. The supernatant was centrifuged at 120,000 g for 30 min at 4 °C and the orange pellet thoroughly resuspended in 22 mL assay buffer. For each reaction, 500 μL of the vesicle preparation was used. For the metal dependence experiments, EDTA was added to a final concentration of 4 mM, the mixture incubated at 4 °C for 5 min, followed by the addition of metal at a concentration of 5 mM and incubation at 4 °C for 5 min. For all experiments, 10 μM prodigiosin (Enzo Life Sciences, 100X stock solution prepared at 1 mM in 20% v/v ethanol in water) was added, the mixture transferred to a round-bottom glass tube

(16 mm × 100 mm) at room temperature. The reaction was started by adding reducing cofactor (NADH, NADPH, (6*R*)- or (6*S*)-tetrhydrobiopterin, or tetrahydrofolate, all from Sigma-Aldrich) at 250 μM, or, in the case of $FMNH_2$, adding FMN to the mixture pre-loaded with a cofactor generation system consisting of glucose-6-phosphate (20mM), 250 μM $NADP^+$, 1 unit/mL glucose-6-phosphate dehydrogenase, and 1 unit/mL NADPH:FMN oxioreductase from *Photobacterium fischeri* (all from Sigma-Aldrich). Enzymatic generation of $FMNH_2$ was necessary because the enzyme is inactivated by sodium dithionite. The *in situ* reduction of FMN to $FMNH_2$ was verified by observing the loss of yellow color. Metal dependence experiments used 250 μM (6*R*)-tetrahydrobiopterin. After shaking at 200RPM at room temperature for 10 min, reactions were quenched using 2 mL 1:1 v/v chloroform:methanol. 500 μL de-ionized water was added, the organic layer evaporated to dryness, dissolved in ethanol, diluted 1:1 with de-ionized water, and analyzed by LC-MRM-MS. Peak areas were calculated using Analyst 1.6.2. To calculate relative enzyme activity, cycloprodigiosin peak areas were normalized to the prodigiosin starting material peak areas to correct for extraction efficiency (< 0.1% conversion had occurred under all conditions), and to a (6*R*)-tetrahydrobiopterin reaction to normalize for enzyme activity differences between vesicle preparations. All conditions shown in Figure 2b, except for $FMNH_2$, were performed in parallel with the same vesicle preparation.

LC-MS acquisition and data analysis

LC-MRM-MS was performed on an AB Sciex 4000 QTRAP with an Agilent 1200 series LC system. 1 μL of sample was injected onto a Phenomenex Kinetex XB-C18 (3 mm × 100 mm) column. Mobile phase: A = 10 mM ammonium formate, brought to pH 4.5 with formic acid, B = methanol buffered identically to A. Method: 35% B for 5 min, ramp from 35% to 80% B in 30 min, 80% B for 8 min, ramp to 35% B in 2 min, re-equilibrate at 35% B for 15 min, all at a flow rate of 200 μL/min. A Turbo Spray V ion source was used in positive ion mode (curtain gas: 20 L/min, temperature: 600 °C, voltage: 4800 V, source gas: 50 L/min, entrance potential: 8 V, collision energy: 45, declustering potential: 45 V, column temperature: 50 °C, Q1 resolution: high, Q3 resolution: unit). The transitions monitored (324→252 for **1**, 322→292 for **2**) were based on published tandem MS spectra[7,30].

LC-TOF-HRMS was performed on an Agilent 1200 series Rapid Resolution HPLC system. Mobile phases were the same as above. 2 μL of sample was injected onto a Phenomenex Kinetex XB-C18 (3 mm × 50 mm) column. Method: 30% B for 8 min, ramp from 30% to 80% B in 20 min, 80% B for 4 min, ramp to 35% B in 1 min, re-equilibrate at 30% B for 7 min, all at a flow rate: 200 μL/min. An Agilent ESI source was used in the positive ion mode (drying gas: 11 L/min, temperature: 325 °C, capillary voltage: 3500 V, nebulizer gas: 25 lb/in^2, fragmentor: 150 V, skimmer: 50 V, declustering potential: 45 V, column temperature: 50 °C, OCT 1 RF Vpp: 170 V).

Semi-quantitative shotgun proteomics

Cell lysis and protein precipitation were performed using a chloroform-methanol extraction as previously described[31]. The protein pellet was re-suspended in 100 mM $(NH_4)HCO_3$ with 20% methanol and the protein concentration was measured using the DC Protein Assay Kit (Bio-Rad). The protein was reduced with 5 mM TCEP for 30 minutes at room temperature,

alkylated with 10 mM iodoacetamide for 30 minutes in the dark at room temperature, and digested with trypsin (1:50 w/w, trypsin:protein) overnight at 37 °C.

Peptide samples (20 μg) were analyzed on an Agilent 6550 iFunnel Q-TOF mass spectrometer coupled to an Agilent 1290 UHPLC system (Agilent Technologies). Peptides were loaded into an Ascentis Express Peptisde ES-C18 column (100 mm × 2.1 mm i.d., 2.7 μm particle size; Sigma Aldrich, St. Louis, MO, USA) operating at 60 °C and flowing at 0.400 mL/min. Mobile phase: A = 0.1% formic acid in water, B = 0.1% formic acid in acetonitrile. Method: 2% B for 2 min, ramp from 2% to 30% B over 30 min, ramp to 50% over 5 min, ramp to 80% over 1 min, hold at 80% B for 7 min, ramp to 2% B over 1 min, hold at 2% B for 4 min. An Agilent Dual Jet Stream Electrospray Ionization source was used in positive-ion mode. Gas temperature: 250 °C, drying gas: 14 L/min, nebulizer: 35 psig, sheath gas temp: 250 °C, sheath gas flow: 11 L/min, VCap: 4,500 V, nozzle voltage: 1,000 V, fragmentor: 180 V, and OCT 1 RF Vpp: 750 V.

The data were acquired with Agilent MassHunter Workstation version B.06.01 and searched against the *P. rubra* genome using Mascot version 2.3.02 (Matrix Science), then filtered and refined using Scaffold version 4.6.1 (Proteome Software Inc.).

Bioinformatics

Pre-aligned Uniprot-RP75 (representative proteome clustered at 75% sequence identity) sequences for the FA_hydroxylase (PF04116) family were obtained directly from Pfam version 3.0[32]. A maximum-likelihood phylogenetic tree was built with Fasttree using default parameters[33]. Branches were assigned colors based on metadata from the Uniprot database[34]. The tree was rendered using iTOL version 3[35].

Data Availability Statement

Strains and plasmids developed for this study (Supplementary Tables 4 and 5) along with annotated sequences, have been deposited in the public instance of the JBEI Registry (https://public-registry.jbei.org/folders/260) and are physically available from the authors and/or Addgene (http://www.addgene.org) upon request. The Department of Energy will provide public access to these results of federally sponsored research in accordance with the DOE Public Access Plan (http://energy.gov/downloads/doe-public-access-plan).

Supplementary Material

Refer to Web version on PubMed Central for supplementary material.

Acknowledgments

We thank Adam Deutschbauer for gifting *E. coli* WM3064. We thank Itay Budin, Jorge Alonso-Gutierrez, Mitchell Thompson, David Fercher, Jesus Barajas, Christopher Eiben, Constance Bailey, Sarah Richardson, Maggie Brown, Megan Garber, Salome Nies, Corey Meadows, Taek Soon Lee, Leonard Katz, and Sara Weschler for helpful discussions, Eduardo de Ugarte for work on the graphical abstract, as well as Susan Gardner, Libby Coyne and Mary Agnitsch for everyday support. We are grateful to ERASynBio (81861: “SynPath”) to J.D.K. the NIGMS (086374) to R.S. and the UC Berkeley SURF Rose Hills fellowship to P.S. for financial support. This work was supported by the DOE Joint BioEnergy Institute and the DOE Joint Genome Institute by the U.S. Department of Energy, Office of Science, Office of Biological and Environmental Research, through contract DE-AC02-05CH11231 between Lawrence Berkeley National Laboratory and the U.S. Department of Energy. The

References

1. Papireddy K, et al. J Med Chem. 2011; 54:5296–5306. [PubMed: 21736388]
2. Stankovic N, Senerovic L, Ilic-Tomic T, Vasiljevic B, Nikodinovic-Runic J. Appl Microbiol Biotechnol. 2014; 98:3841–3858. [PubMed: 24562326]
3. Williamson NR, et al. Future Microbiol. 2007; 2:605–618. [PubMed: 18041902]
4. Montaner B, Pérez-Tomás R. Life Sci. 2001; 68:2025–2036. [PubMed: 11388704]
5. Yamamoto C, et al. Hepatology. 1999; 30:894–902. [PubMed: 10498640]
6. Jones BT, Hu DX, Savoie BM, Thomson RJ. J Nat Prod. 2013; 76:1937–1945. [PubMed: 24053736]
7. Lee JS, et al. Appl Environ Microbiol. 2011; 77:4967–4973. [PubMed: 21642414]
8. Sydor PK, et al. Nat Chem. 2011; 3:388–392. [PubMed: 21505498]
9. Salem SM, et al. J Am Chem Soc. 2014; 136:4565–4574. [PubMed: 24575817]
10. Withall DM, Haynes SW, Challis GL. J Am Chem Soc. 2015; 137:7889–7897. [PubMed: 26023709]
11. Kimata S, Izawa M, Kawasaki T, Hayakawa Y. J Antibiot. 2017; 70:196–199. [PubMed: 27460763]
12. Kancharla P, Lu W, Salem SM, Kelly JX, Reynolds KA. J Org Chem. 2014; 79:11674–11689. [PubMed: 25380131]
13. Hu DX, Withall DM, Challis GL, Thomson RJ. Chem Rev. 2016; 116:7818–7853. [PubMed: 27314508]
14. Williamson NR, Fineran PC, Leeper FJ, Salmond GPC. Nat Rev Microbiol. 2006; 4:887–899. [PubMed: 17109029]
15. Xie BB, et al. J Bacteriol. 2012; 194:1637–1638. [PubMed: 22374963]
16. Williamson NR, et al. Mol Microbiol. 2005; 56:971–989. [PubMed: 15853884]
17. Shanklin J, Guy JE, Mishra G, Lindqvist Y. J Biol Chem. 2009; 284:18559–18563. [PubMed: 19363032]
18. Bai Y, et al. Nature. 2015; 524:252–256. [PubMed: 26098370]
19. Tang MC, Zou Y, Watanabe K, Walsh CT, Tang Y. Chem Rev. 2017; 117:5226–5333. [PubMed: 27936626]
20. Watschinger K, Werner ER. IUBMB Life. 2013; 65:366–372. [PubMed: 23441072]
21. Watschinger K, et al. Biochem J. 2012; 443:279–286. [PubMed: 22220568]
22. Futai M. J Membr Biol. 1974; 15:15–28. [PubMed: 4152065]
23. Mayer M, et al. Pteridines. 2013; 24
24. Chawrai SR, Williamson NR, Mahendiran T, Salmond GPC, Leeper FJ. Chem Sci. 2012; 3:447–454.
25. Barry SM, Challis GL. ACS Catal. 2013; 3:2362–2370.
26. Johnson RE, de Rond T, Lindsay VNG, Keasling JD, Sarpong R. Org Lett. 2015; 17:3474–3477. [PubMed: 26114660]
27. Dairi K, Tripathy S, Attardo G, Lavallée JF. Tetrahedron Lett. 2006; 47:2605–2606.
28. Hillson NJ, Rosengarten RD, Keasling JD. ACS Synth Biol. 2012; 1:14–21. [PubMed: 23651006]
29. Wang P, et al. Microb Cell Fact. 2015; 14:11. [PubMed: 25612661]
30. Alihosseini F, Lango J, Ju KS, Hammock BD, Sun G. Biotechnol Prog. 2010; 26:352–360. [PubMed: 19902486]
31. Batth TS, Keasling JD, Petzold CJ. Methods Mol Biol. 2012; 944:237–249. [PubMed: 23065621]
32. Finn RD, et al. Nucleic Acids Res. 2014; 42:D222–30. [PubMed: 24288371]
33. Price MN, Dehal PS, Arkin AP. Mol Biol Evol. 2009; 26:1641–1650. [PubMed: 19377059]
34. UniProt Consortium. Nucleic Acids Res. 2015; 43:D204–12. [PubMed: 25348405]

35. Letunic I, Bork P. Nucleic Acids Res. 2016; 44:W242–5. [PubMed: 27095192]

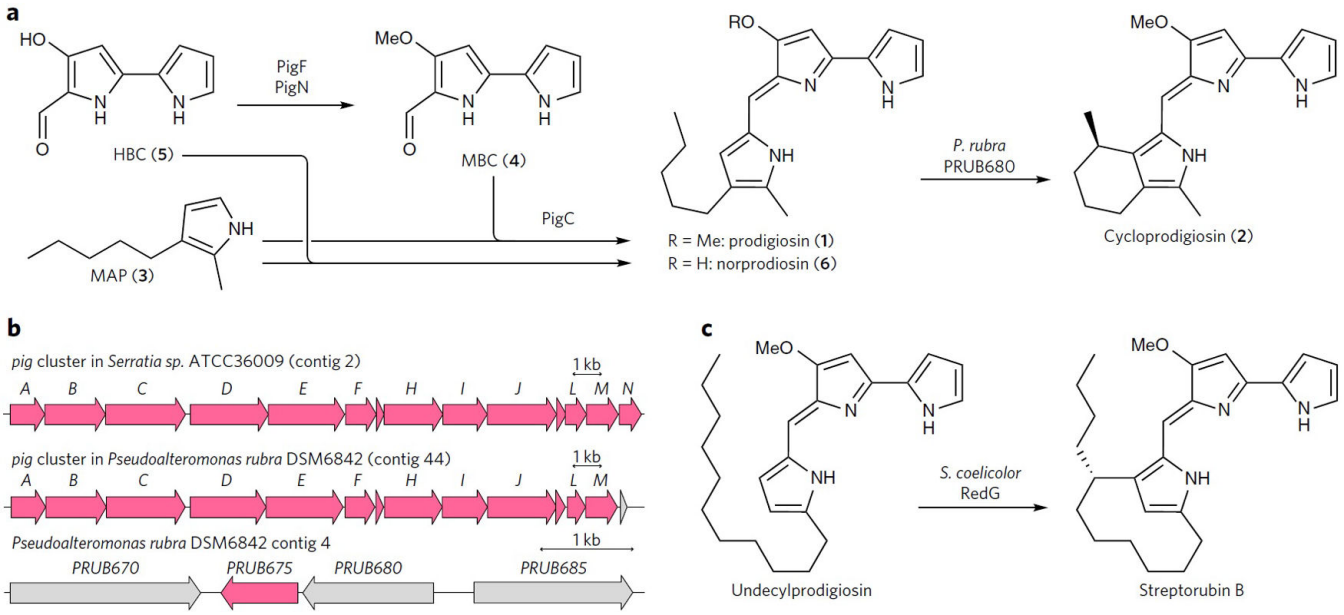

Figure 1. Biosynthesis of prodiginines in P. rubra compared to that in other organisms

(**a**) Hypothetical prodigiosin (**1**) biosynthetic pathway in *P. rubra* (by analogy to the pathway elucidated in *Serratia*) and the cyclization of **1** into cycloprodigiosin (**2**) investigated in this work. (**b**) Comparison of the *pig* gene cluster in *Serratia*, which produces only **1**, and *P. rubra*, which produces both **1** and **2**, shows that *pigN* is absent in the latter. The gene downstream of *pigM* in *P. rubra* shows no similarity to *pigN*. Also shown is an excerpt of *P. rubra* contig 4, which contains *PRUB675* and *PRUB680*. Genes in pink have homology to *Serratia pig* genes and/or to *Streptomyces red* genes. (**c**) The Rieske monooxygenase-like RedG catalyzes the carbocyclization of undecylprodigiosin to form streptorubin B, motivating our search for the enzyme responsible for the analogous cyclization of **1** in *P. rubra*.

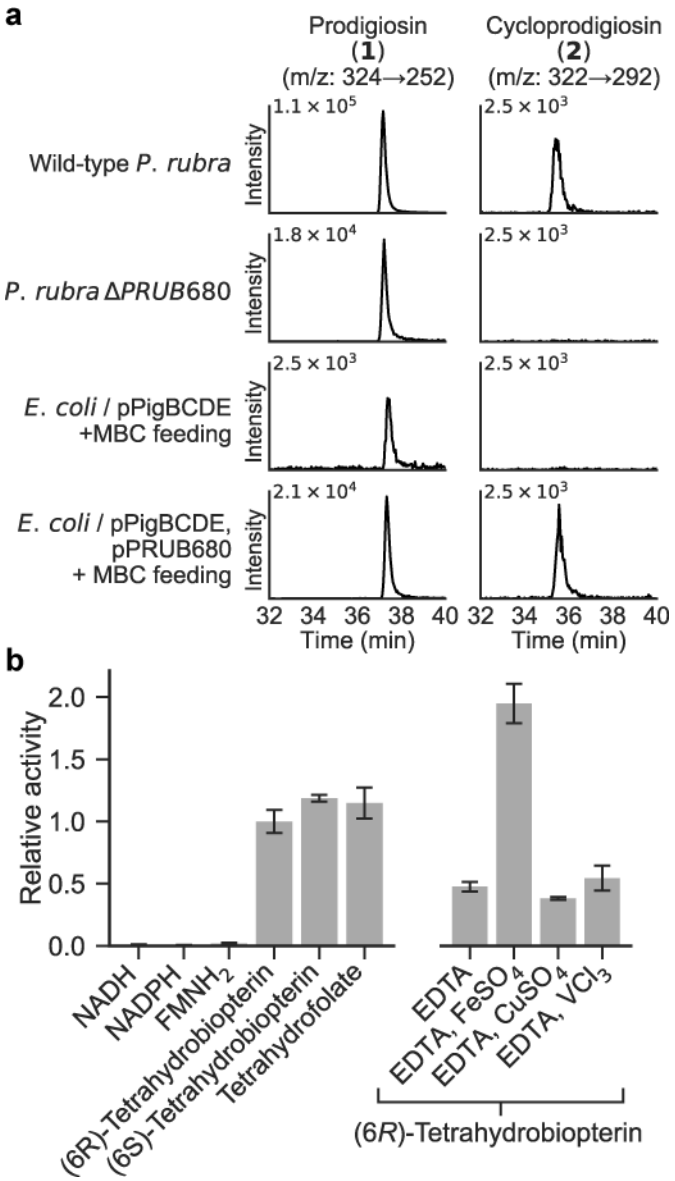

Figure 2. Analysis of prodigiosin cyclization *in vivo* and *in vitro*

(**a**) *In vivo* production of prodiginines. For experiments in *E. coli*, the cells were fed MBC (**4**), which is turned into prodigiosin (**1**) by PigBCDE. **1** is in turn converted to cycloprodigiosin (**2**) by PRUB680 if present. For standards, see Supplementary Figure 1. (**b**) *In vitro* experiments with PRUB680 in inverted *E. coli* membrane vesicles. Vesicles were shaken with 10 μM 1 in the presence of the indicated cofactors (left). Reactions were initiated by addition of 250 μM reducing cofactor. For metal dependency experiments (right), vesicles were incubated with 4 mM EDTA, followed by 5 mM metal ion, before initiating the reaction with 250 μM (6*R*)-tetrahydrobiopterin. Error bars represent s.d. of triplicates.